J Mol Model (2005) 12: 42–48
DOI 10.1007/s00894-005-0002-1

ORIGINAL PAPER

Karisa Karla Manhani · Helen Andrade Arcuri
Nelson José Freitas da Silveira · Hugo Brandão Uchôa
Walter Filgueira de Azevedo Jr · Fernanda Canduri

Molecular models of protein kinase 6 from *Plasmodium falciparum*

Received: 16 December 2004 / Accepted: 1 July 2005 / Published online: 4 November 2005

Abstract Cyclin-dependent kinases (CDKs) have been identified as potential targets for development of drugs, mainly against cancer. These studies generated a vast library of chemical inhibitors of CDKs, and some of these molecules can also inhibit kinases identified in the *Plasmodium falciparum* genome. Here we describe structural models for Protein Kinase 6 from *P. falciparum* (PfPK6) complexed with Roscovitine and Olomoucine. These models show clear structural evidence for differences observed in the inhibition, and may help designing inhibitors for PfPK6 generating new potential drugs against malaria.

Keywords Kinases · Bioinformatics · *Plasmodium falciparum* · Roscovitine · Olomoucine

Introduction

Unicellular parasites such as *Plasmodium falciparum* (malaria), *Leishmania major* (leishmaniosis), *Trypanosoma brucei* (sleeping sickness), *Trypanosoma cruzi* (Chagas disease) and *Toxoplasma gondii* (toxoplasmosis) are responsible for the world's most widespread diseases. These microrganisms have genuine cyclin-dependent kinases (CDKs or CDK)-related kinases. Several *P. falciparum* genes encoding cdc2-related protein kinases have been identified, but the modalities of their regulation remain largely unexplored. [1, 2].

Malaria remains a major and growing threat to the public health and economic development of countries in the tropical and subtropical regions of the world. Approximately 40% of the world's population live in areas where malaria is endemic. There are an estimated 300–500 million cases and up to 2.7 million deaths from malaria each year. The mortality levels are greatest in sub-Saharan Africa, where children under 5 years of age account for 90% of all deaths due to malaria [1, 2]. Human malaria is caused by infection with intracellular parasites of the genus *Plasmodium* (parasite) that is transmitted by *Anopheles gambiae* mosquitoes. Among four species of *Plasmodium* that infect humans, *P. falciparum* is the most lethal [3].

While the stages of parasitic infection are well documented, until recently, little has been known concerning the regulation of the parasitic life cycle. However, the identification of a family of kinases from *P. falciparum* with a high degree of sequence conservation to the mammalian CDKs has allowed researchers to begin investigation of the mechanisms that control passage through the parasitic life cycle. *P. falciparum* Protein Kinase 5, PfPK5, was isolated in 1994 using oligonucleotides based on the sequences of CDK2 and CDK1 [4, 5]. In a sequence comparison with members of the human CDK family, it shares the greatest degree of sequence identity (about 60%) with human CDK1 and CDK5. The similarity between PfPK5 and the mammalian CDKs in terms of their mechanism of kinase activation and inhibition has led researchers to investigate the effects of known small-molecule CDK inhibitors on the growth of *P. falciparum* [4]. The PfPK5 structure was recently determined (PDB code: 1OB3) [6].

In addition to the observed sequence conservation, evidence suggests that PfPK5 is activated in a manner similar to the activation of the mammalian CDKs. First, research into the mechanism of PfPK5 activation demonstrates the necessity of Thr158 phosphorylation of PfPK5 for activation [7]. Similar phosphorylation events have been shown to be necessary for the activation of the mammalian CDKs. For example, activation of CDK2 requires phosphorylation of Thr160 [8]. Second, the in vitro activation of PfPK5 is enhanced as a result of co-incubation with the human cyclins [3]. Full activation

K. K. Manhani · H. A. Arcuri · N. J. F. da Silveira
H. B. Uchôa · W. F. de Azevedo Jr · F. Canduri (✉)
Departamento de Física, Universidade Estadual Paulista,
UNESP, Rua Cristovão Colombo, 2265, 15054-000
São José do Rio Preto, São Paulo, Brasil
E-mail: canduri@webmail.ibilce.unesp.br
Tel.: +55-017-2212463
Fax: +55-017-2212247

of the mammalian CDKs requires the association of the catalytic kinases with a regulatory cyclin subunit [9]. These data strongly suggest a role for PfPKs in the life cycle of *P. falciparum* similar to that observed for CDK2 in the mammalian cell cycle [4].

PfPK6 was recently isolated by differential display RT-PCR (DDRT-PCR) of mRNA obtained from different asexual erythrocytic stages of *P. falciparum*, which shows sequence similarity to CDK [10]. Overexpression of PfPK6 in *Escherichia coli* allowed the biochemical properties of the recombinant enzyme to be studied. In addition, immunolocalization and immunoblot analysis were performed to localize the PfPK6 protein in various developmental stages [10]. Kinases are often characterized by their sensitivity to specific diagnostic inhibitors. Several specific inhibitors of CDKs have been described, of which roscovitine [2-(1-d,l-hydroxymethylpropylamino)-6-benzylamino-9-isopropylpurine] and olomoucine [2-(2-hydroxyethylamino)-6-benzylamino-9-methylpurine] show remarkable selectivities for some of the members of the cdc2-related kinases [10, 11]. Increasing the concentration of both olomoucine and roscovitine causes the progressive inhibition of autophosphorylation of PfPK6 in a kinase assay in vitro. However, the IC_{50} value for roscovitine (30 μM) is one-sixth that of olomoucine (180 μM) [10].

Since no structural study of PfPK6 exists, this article describes three-dimensional models of PfPK6 in complex with roscovitine and olomoucine, by applying computational homology-modeling techniques and utilizing the high-resolution crystal structure of CDK2 as template. The structural features of ATP-binding sites of PfPK6 and CDK2 were compared in order to gain further insight into the structural basis for chemical inhibition of CDKs.

Methods

Molecular modeling

Homology modeling is usually the method of choice when there is a clear relationship of homology between the sequence of a target protein and at least one known structure. Model building of the complexes was carried out using the program Parmodel [12], which is a web server for automated modeling and protein structural assessment. Parmodel runs a parallelized version of MODELLER [13]. MODELLER is an implementation of an automated approach to comparative modeling by satisfaction of spatial restraints. The modeling procedure begins with alignment of the sequence to be modeled (target) with the sequence of related known three-dimensional structures in complex with the inhibitor (templates). This alignment is usually the input to the program. The output is a three-dimensional model for the target sequence containing all main-chain and side-chain nonhydrogen atoms [13].

The homology models of PfPK6 with inhibitors were based on the atomic coordinates of CDK2 complexed with roscovitine and olomoucine. The alignment of CDK2 (template) and PfPK6 (target) is shown in Fig. 1.

The modeling was performed in the presence of inhibitors from the template. These inhibitors were refined in the active site of the models. Several slightly different models can be calculated by varying the initial structure. A total of 1000 models were generated by the program Parmodel [12], the final model was select based on stereochemical quality. All optimization process was performed on a Beowulf cluster with 16 nodes (Bio-Comp, AMD Athlon XP 2100+).

Analysis of the model

The overall stereochemical quality of the final models PfPK6 complexed with roscovitine and olomoucine was assessed by the program PROCHECK [14]. The cutoff for hydrogen bonds and salt bridges was 3.4 Å. The contact surfaces for the binary complexes were calculated using AREAIMOL and RESAREA [15].

For superposition of Cα, we used the program LSQKAB from CCP4 [15]. The root mean square deviations (RMSD) from ideal geometries for bond lengths, bond angles, dihedrals and impropers were calculated with X-PLOR [16]. The program VERIFY-3D was used to assess structural quality of the homology models [17, 18]. G-factor values were calculated using PROCHECK [14].

Results and discussion

Quality of the model

The analysis of the Ramachandran plots for the templates and models indicates that over 90% of the residues are in the most favorable regions. Analysis of the structural quality of the homology models using PROCHECK [14], XPLOR [16] (for RMSD from ideal geometry), and VERIFY-3D [17, 18] strongly indicates that the models are good enough for structural studies (Table 1).

Overall description and interactions with inhibitors

The models for *P. falciparum* Protein Kinase complexed with inhibitors are folded into the typical bilobal structure, with the smaller N-terminal lobe consisting predominantly of β-sheet structures and the larger C-terminal lobe consisting primarily of α-helices. The N-terminal lobe of PfPK6, as observed for CDKs, consists of a sheet of five antiparallel β-strands (β1–β 5) and a single large helix (α1).The C-terminal lobe contains a pseudo-4-helical bundle (α 2, 3, 4, 6) a small β-ribbon (β 6 –β 8) and two additional helices (α 5, 7).

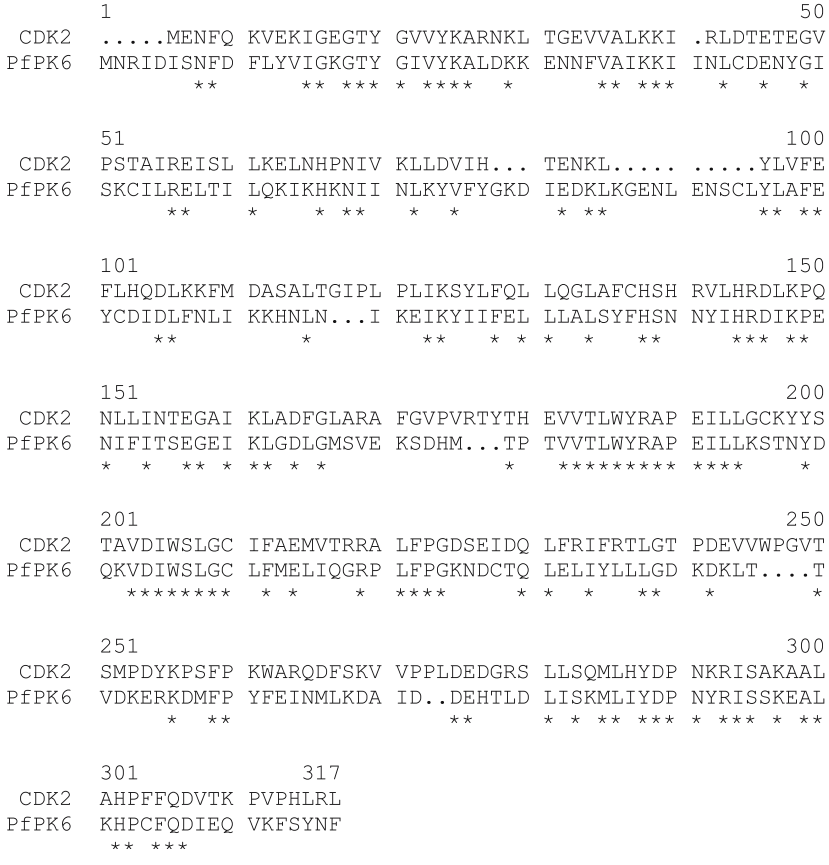

Fig. 1 Sequence alignment of CDK2 with PfPK6 (39.7% of identity). The alignment was performed with the program MULTALIN [28]

Table 1 Analysis of the stereochemical quality, 3D PROFILE and average G-factor values for the PfPK6 model

Complex	Region of the Ramachandran plot				Analysis structural		
	Most favorable (%)	Additional allowed (%)	Generously allowed (%)	Disallowed (%)	3D Profile[a]	G Factor	
						Main chain covalent forces	Dihedral angles
CDK1-Rosc	87.8	10.7	1.5	0.0	0.97S	−0.23	−0.27
CDK1-Olo	95.0	4.6	0.4	0.0	0.89S	−0.26	−0.04
CDK5-Rosc	90.2	7.8	3.0	2.0	0.93S	−0.32	−0.07
CDK5-Olo	93.4	6.2	0.4	0.0	0.87S	−0.23	−0.03
PfPK6-Rosc	91.3	6.3	2.0	0.4	0.80S	−0.28	−0.11
PfPK6-Olo	91.3	6.7	1.6	0.4	0.76S	−0.29	−0.12
CDK2-Rosc	87.1	12.9	0.0	0.0	0.98S	−0.45	−0.48
CDK2-Olo	89.6	10.4	0.0	0.0	1.06S	−0.37	−0.05

[a] Ideally, scores should be above −0.5. Values below −1.0 may need investigation

Fig. 2 shows schematic drawings of the complex PfPK6-roscovitine and PfPK6-olomoucine. The roscovitine and olomoucine molecules are found in the cleft between the two lobes. The core (the β-sheet and the helical bundle) of the CDK1, CDK5 and PfPK6 structures are very similar to that of CDK2 [19–24].

The larger differences between the structures of CDK2 and PfPK6 are in the loops 85–94; 107–119; 164–174 and 237–262 of the regions of PfPK6, which are also observed in the alignment of primary sequences (Fig. 1).

The specificity and affinity between enzyme and its inhibitor depend on directional hydrogen bonds and ionic interactions, as well as on shape complementarity of the contact surfaces of the two partners [21–23, 25, 26]. Superpositions of the CDK2-ATP onto CDK1, CDK5 and PfPK6 structures complexed with roscovitine and olomoucine indicate that the two ring systems of roscovitine with ATP and olomoucine with ATP overlap approximately in the same plane [21–24, and 27]; however, with different orientations. As observed in the crystallographic structures of CDK2-roscovitine and CDK2-olomoucine, the region of CDK1, CDK5 and PfPK6 occupied by the phenyl rings of roscovitine and olomoucine are pointing away from the ATP-binding

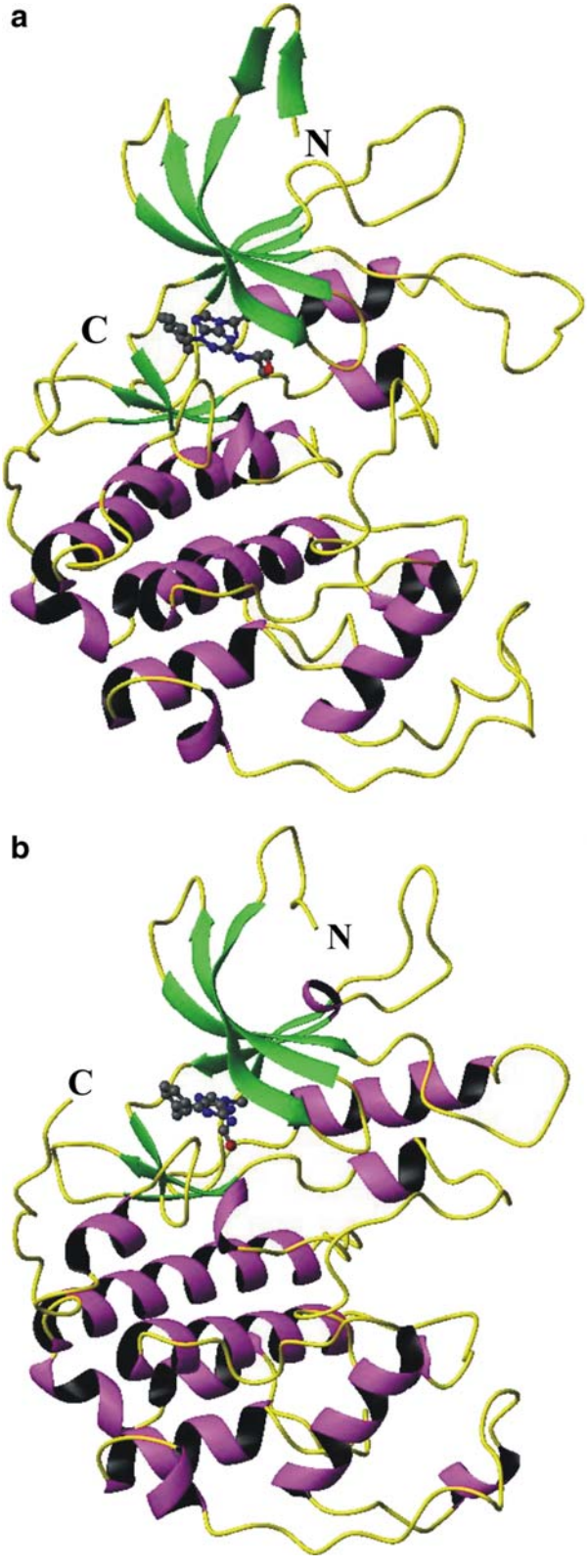

Fig. 2 Ribbon diagram of PfPK6 complexed with **a** roscovitine and **b** olomoucine. Figures were generated by MolMol [29]

pocket, and partially exposed to solvent in the both complexes.

For the complexes CDK2-roscovitine and CDK2-olomoucine, the contact areas between inhibitor and CDK2 are 320 and 269 Å^2, respectively. This analysis was used for comparison of the CDK1, CDK5 and PfPK6 complexed with the same ligands. Table 2 summarizes some structural results and IC50 values.

Interactions of roscovitine and olomoucine with PfPK6

The active site of PfPK6 is structurally similar to the CDKs. Two hydrogen bonds between PfPK6 and inhibitors, involving the residue Leu95, were observed for the binary complexes. Table 3 shows the intermolecular hydrogen bonds for the structures of PfPK6, CDK1, CDK2 and CDK5. Figure 3a, b show the binding pocket for PfPK6-Roscovitine and PfPK6-olomoucine complexes, and Fig. 4 shows the superposition among them, and the CDK2 template.

The contact areas for the complexes of PfPK6 with roscovitine and PfPK6 with olomoucine are 356 and 297 Å^2, respectively (Table 1), compatible with the values observed to CDK2-roscovitine and CDK2-olomoucine complexes. However, IC50 is higher for PfPK6 than for CDK2. The structural basis for this higher IC50 relies on the presence of two tyrosine residues in the entry of the ATP-binding pocket observed in the complex PfPK6-roscovitine and PfPK6-olomoucine (Fig. 3a, b). This pair of tyrosines is not observed in the CDK2 complexes. We suggest that these tyrosines offer further hindrance to the docking of roscovitine and olomoucine to the ATP-binding pocket of PfPK6, justifying the higher IC50 observed for the inhibition of PfPK6 by roscovitine and olomoucine (30 and 180 μM, respectively) [10], when compared with the inhibition of CDK2 (0.7 and 7 μM, respectively) [10]. The values of contact area to CDK1 and CDK5 are in agreement with the IC50 values. The RMSD values from the ideal geometry of PfPK6 and CDKs 1, 2 and 5 are shown in Table 4.

Conclusion

Analysis of the charge distribution of the binding pockets indicates the presence of charge and shape complementary between CDK1 complexed with rosco-

Table 2 Summary of structural and function results

Complex	IC50 (μM)	Contact area (Å^2)	Number of intermolecular hydrogen bonds
CDK1-Rosc	0.45	339	6
CDK1-Olo	7	285	2
CDK5-Rosc	0.16	334	5
CDK5-Olo	3	289	2
CDK2-Rosc	0.7	320	2
CDK2-Olo	7	269	2
PfPK6-Rosc	30	356	2
PfPK6-Olo	180	297	2

Table 3 Intermolecular hydrogen bonds

Protein	Residues	Inhibitor	Distance (Å)
CDK1-Roscovitine	Leu83N	N7	3.4
	Leu83O	N6	3.1
	Gln132NL2	O1	2.8
	Asp86OD2	N1	3.2
	Asp86OD2	N2	3.3
CDK2-Roscovitine	Leu83N	N7	3.4
	Leu83O	N6	2.8
CDK5-Roscovitine	Cys83N	N7	3.5
	Cys83O	N6	3.1
	Gln130NE2	O1	3.3
	Asp86OD2	N2	3.5
	Asp86OD2	N1	3.2
CDK1-Olomoucine	Leu83N	N7	2.9
	Leu83O	N6	2.6
CDK2-Olomoucine	Leu83N	N7	2.9
	Leu83O	N6	2.6
CDK5-Olomoucine	Cys83N	N7	2.9
	Cys83O	N6	2.6
PfPK6-Roscovitine	Leu95N	N7	3.4
	Leu95O	N6	2.8
PfPK6-Olomoucine	Leu95N	N7	2.9
	Leu95O	N6	2.8

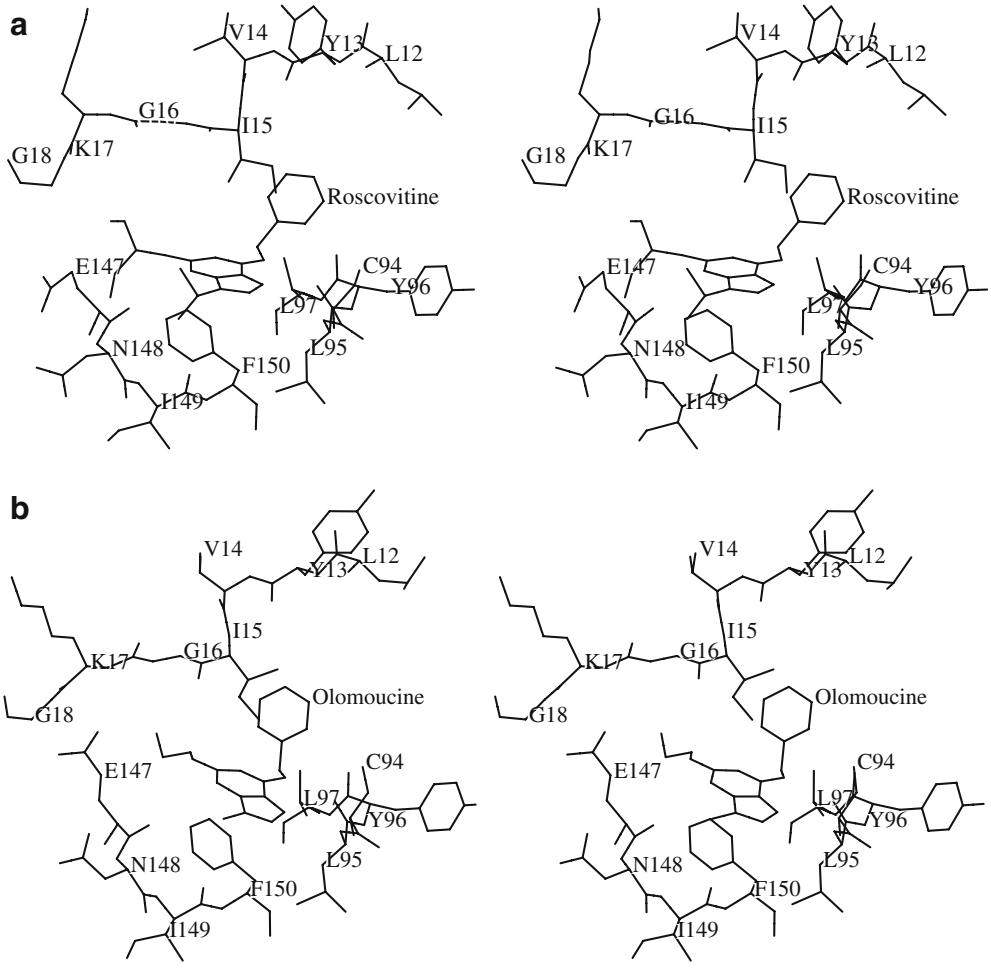

Fig. 3 Stereo view of binding pocket of the PfPK6 in complex with **a** roscovitine and **b** olomoucine

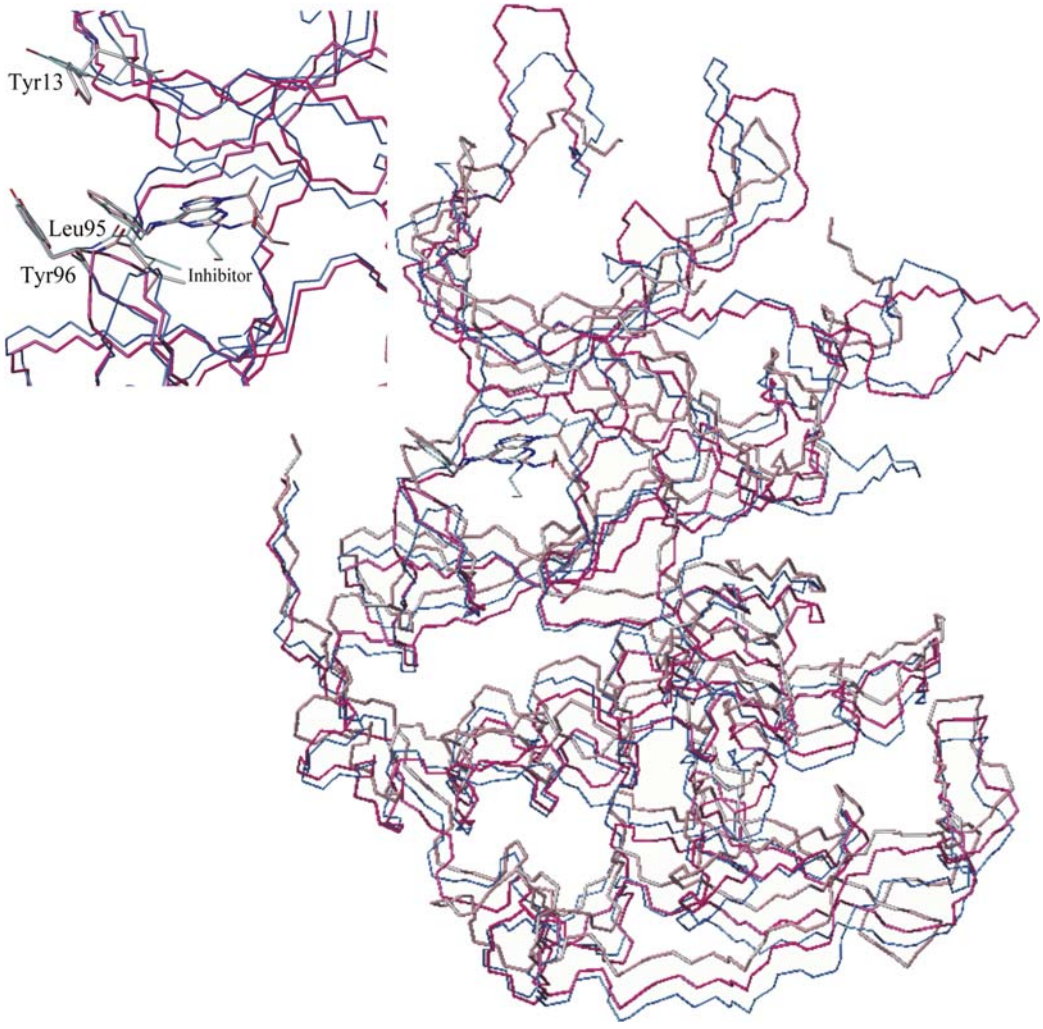

Fig. 4 Superposition of the complexes PfPK6-roscovitine (in *pink*) and PfPK6-olomoucine (in *blue*), with CDK2 (in *light pink*). In detail is shown the active site with the tyrosine residues. Figures were generated by MolMol [29]

Table 4 Summary of the RMSD values from ideal geometry for the complexes

Complex	Bonds lengths (Å)	Bond angles (degrees)	Dihedrals (degrees)
CDK1-Roscovitine	0.021	2.273	24.404
CDK1-Olomoucine	0.019	2.728	23.396
CDK5-Roscovitine	0.042	3.224	24.294
CDK5-Olomoucine	0.019	3.074	23.516
PfPK6-Roscovitine	0.018	3.295	23.283
PfPK6-Olomoucine	0.021	3.328	23.403
CDK2-Roscovitine	0.240	2.256	26.911
CDK2-Olomoucine	3.389	3.242	24.790

vitine, CDK5 complexed with roscovitine and PfPK6 complexed with roscovitine and olomoucine. Figure 5a, b show the electrostatic potential surface of the structures of PfPK6 compared with CDK2. Analysis of the present structural models indicates that roscovitine and olomoucine are more specific for CDK1, CDK2 and CDK5 than for PfPK6.

Significant difference was observed in the PfPK6 models in complex with roscovitine and olomoucine. These models present a pair of tyrosines, which make a barrier for the ligand (Fig. 3a, b). The presence of Tyr13 and Tyr96 in the entrance of the ATP-binding pocket reduces the volume available for ligand binding in the PfPK6 active site (Fig. 4). The presence of this pair of tyrosines is the structural basis for the high values of IC50 for PfPK6 when compared with CDK1, CDK2 and CDK5. Further inhibition experiments may confirm this hypothesis.

The atomic coordinates for the homology models can be retrieved from the Homology Model Database (http://www.biocristalografia.df.ibilce.unesp.br/tools/hmdb/index.php) (access codes: 1PFPK6 for PfPK6-roscovitine and 2PFPK6 for PfPK6-Olomoucine).

Acknowledgments This work was supported by grants from FAPESP (SMOLBNet 01/07532-0, 02/04383-7, 04/00217-0), CNPq, CAPES and Instituto do Milênio (CNPq-MCT). WFA (CNPq, 300851/98-7) is researcher for Brazilian Research Council (CNPq).

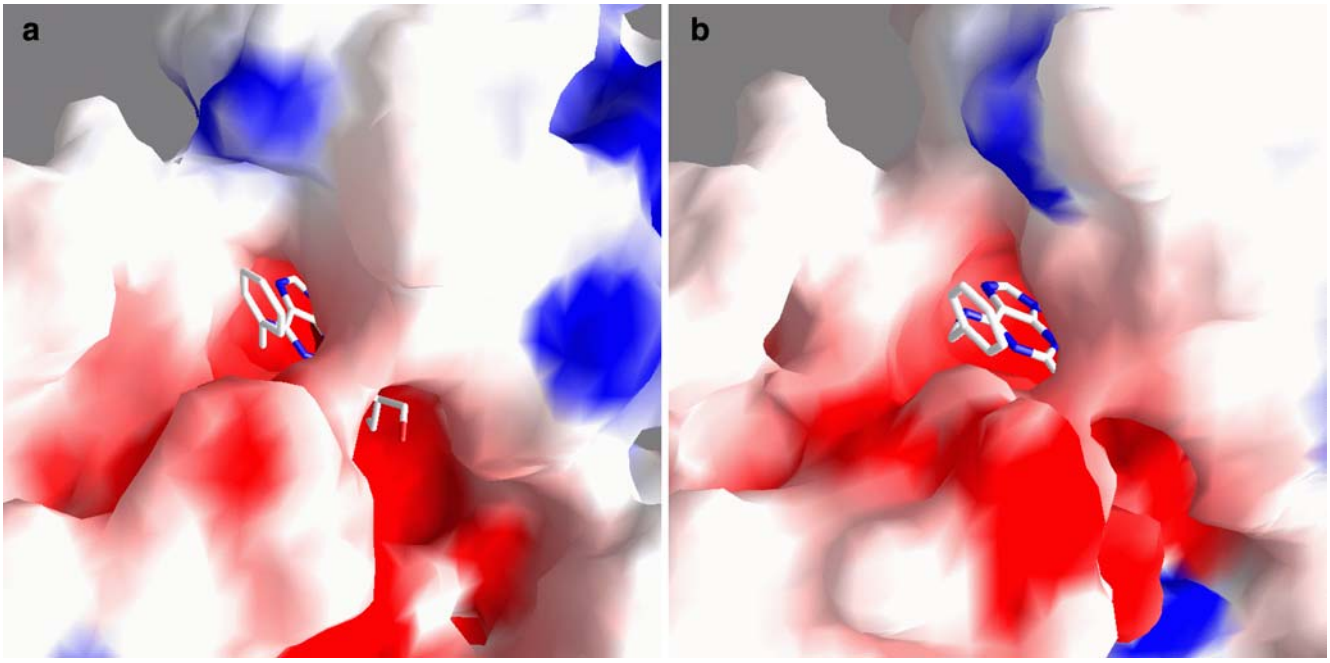

Fig. 5 Electrostatic potential surfaces for ATP binding pocket of **a** PfPK6-roscovitine and **b** PfPK6-olomoucine. Figures were generated with GRASP [30] shown from −10 to + 10 kT. Uncharged regions are white. It is shown only part of inhibitor due to tyrosines in the entrance

References

1. Doerig C, Meijer L, Mottram JC (2002) Trends Parasitol 18:366–371
2. Ward P, Equinet L, Packer J, Doerig C (2004) BMC Genomics 5:79–97
3. le Roch K, Sestier C, Dorin D, Waters N, Kappes B, Chakrabarti D, Meijer L, Doerig C (2000) J Biol Chem 275:8952–8958
4. Keenan SM, Welsh WJ (2004) J Mol Graph Model 22:241–247
5. Gardener MJ, Hall N, Fung E, White O, Berriman M, Hyman RW, Carlton JM, Pain A, Nelson KE, Bowman S, Paulsen IT, James K, Eisen JA, Rutherford K, Salzberg SL, Craig A, Kyes S, Chan M-S, Nene V, Shallom SJ, Suh B, Peterson J, Angiuoli S, Pertea M, Allen J, Selengut J, Haft D, Mather MW, Vaidya AB, Martin DMA, Fairlamb AH, Fraunholz MJ, Roos DS, Ralph SA, McFadden GI, Cummings LM, Subramanian GM, Mungall C, Venter JC, Carucci DJ, Hoffman SL, Newbold C, Davis RW, Fraser CM, Barrell B (2002) Nature 419:498–511
6. Holton S, Merckx A, Burgess D, Doerig C, Noble M, Endicott J (2003) Structure 11:1329–1337
7. Graeser R, Franklin RM, Kappes B (1996) Mol Biochem Parasitol 79:125–127
8. Gu Y, Rosenblatt J, Morgan DO (1992) EMBO J 11:3995–4005
9. Sherr CJ (1996) Science 274:1672–1677
10. Bracchi-Ricard V, Barik S, DelVecchio C, Doerig C, Chakrabarti R, Chakrabarti D (2000) Biochem J 347:255–263
11. Meijer L (1996) Trends Cell Biol 6:393–397
12. Uchoa HB, Jorge GE, da Silveira NJ, Camera JC, Canduri F, De Azevedo WF (2004) Biochem Biophys Res Commun 325:1481–1486
13. Sali A, Blundell TL (1993) J Mol Biol 234:779–815
14. Laskowski RA, MacArthur MW, Smith DK, Jones DT, Hutchinson EG, Morris AL, Naylor D, Moss DS, Thorton JM (1994) PROCHECK v.3.0—Program to check the stereochemistry quality of Protein structures—Operating instructions
15. Collaborative Computational Project No 4 (1994) Acta Crystallogr D50:760–763
16. Brünger AT (1992) X-PLOR Version 3.1: a system for crystallography and NMR. Yale University Press, New Haven
17. Lüthy R, McLachlan AD, Eisenberg D (1991) Proteins 10:229–239
18. Bowie JU, Lüthy R, Eisenberg D (1991) Science 253:164–170
19. de Azevedo Jr WF, Leclerc S, Meijer L, Havlicek L, Strnad M, Kim S-H (1997) Eur J Biochem 243:518–526
20. de Azevedo Jr WF, Mueller-Dieckmann, HJ, Schulze-Gahmen U, Worland PJ, Sausville E, Kim S-H (1996) Proc Natl Acad Sci USA 93:2735–2740
21. Canduri F, Uchoa HB, de Azevedo Jr WF (2004) Biochem Biophys Res Commun 324:661–666
22. de Azevedo WF Jr, Gaspar RT, Canduri F, Camera JC Jr, da Silveira NJF (2002) Biochem Biophys Res Commun 297:1154–1158
23. Canduri F, de Azevedo WF Jr (2005) Curr Computer-Aided Drug Design 1:53–64
24. Taylor SS, Radzio-Andzelm E (1994) Structure 2:345–55
25. de Azevedo WF Jr, Canduri F, Fadel V, Teodoro LGVL, Hial V, Gomes RAS (2001) Biochem Biophys Res Commun 287:277–281
26. Canduri F, Teodoro LGVL, Lorenzi CCB, Hial V, Gomes RAS, Ruggiero Neto J, de Azevedo WF Jr (2001) Acta Crystallogr D57:1560–1570
27. Schulze-Gahmen U, Brandsen J, Jones HD, Morgan DO, Meijer L, Vesely J, Kim S-H (1995) Proteins 4:378–391
28. Corpet F (1988) Nucl Acids Res 16:10881–10890
29. Koradi R, Billeter M, Wüthrich K (1996) J Mol Graphics 14:51–55
30. Nicholls A, Sharp KA, Honig B (1991) Proteins 11:281–296